Gulf Journal of Mathematics
Vol 24, Issue 2 (2026) 1-25

ISSN: 2309-4966
https://doi.org/10.56947/4t8yjn31

A DELAYED TWO-STRAIN EPIDEMIC MODEL ON COMPLEX NETWORKS

HAKIM HABRI[1*], AMINE EL KOUFI[12] and BRAHIM FAHID[12]

Abstract. Complex networks provide a realistic framework for describing disease transmission by accounting for the heterogeneous contact patterns observed in real populations. Motivated by this feature, we propose a two-strain epidemic model with nonlinear saturated incidence rates and two time delays on complex networks. We first establish the well-posedness of the model by proving the positivity and boundedness of its solutions. Next, we derive the equilibrium points and characterize their existence. By constructing appropriate Lyapunov functionals, we obtain sufficient conditions for the global asymptotic stability of each equilibrium. Finally, we perform numerical simulations to confirm the theoretical results.

Keywords. Complex network, epidemic model, global stability, Lyapunov function
2020 Mathematics Subject Classification. Primary 92D30; 37N25; Secondary 34K20; 05C82

1. Introduction

Infectious diseases arising from genetic mutations in pathogens represent a major threat to human health and remain a significant global concern[14]. Genetic mutations can lead to new strains with enhanced transmissibility, increased resistance to treatment, or altered clinical characteristics. For example, influenza viruses have generated several strains, including H1N1 and H3N2 [13, 33]. Similarly, tuberculosis has evolved into drug-resistant forms, notably multidrug-resistant tuberculosis (MDR-TB) and extensively drug-resistant tuberculosis (XDR-TB)[11, 10]. More recently, the world has also faced an emerging variant of the SARS-CoV-2 virus, known as COVID-19 [43].
Mathematical modeling provides a powerful framework for understanding the transmission dynamics of infectious diseases and for evaluating effective control and prevention strategies [49]. Such models are commonly formulated using ordinary differential equations (ODEs), which describe the temporal evolution of

Date: Received: Aug 3, 2026; Revised: Sep 1, 2026; Accepted: Sep 8, 2026.
* Corresponding author
© The Author(s) 2026. This article is licensed under a Creative Commons Attribution-NonCommercial-NoDerivatives 4.0 International License. To view a copy of the licence, visit https://creativecommons.org/licenses/by-nc-nd/4.0/.

different epidemiological compartments. One of the earliest and most influential compartmental models is the SIR model, introduced in[16]. Since then, numerous extensions have been developed to account for different epidemiological characteristics, including the SIS [38], SIRS [44], and SEIR models [25].
Regarding disease transmission, infection incidence is an essential element for analyzing the transmission of contagious diseases. Several researchers have suggested different incidence functions, including bilinear and nonlinear forms [3, 4, 18]. The bilinear incidence of the form βSI has been commonly used in the modeling of diseases. However, at high infective levels, the frequency of successful interactions between infected and susceptible individuals does not continue to increase as suggested by the bilinear incidence rate, but reaches a saturation level due to the crowding effect or due to the public health response. This phenomenon was considered in the research presented by Capasso and Serio in [5], they introduced the nonlinear incidence rate $S\varphi(I) = \dfrac{\beta SI}{1+\alpha I}$, where $\varphi(I)$ approaches a saturation level when I grows large, which can be used to explain the practical phenomenon. Furthermore, epidemic models that use the nonlinear incidence rate can exhibit qualitatively different dynamical behaviors [29, 2], which are more consistent with reality than other epidemic models.
In general, classical models based on the homogeneous mixing assumption cannot investigate the effect of heterogeneity within a population, which prevents a realistic representation of social networks in which individuals have different numbers of connections. As a result, these models are often unsuitable for simulating the spread of diseases in situations where such dynamics are strongly influenced by network topology and connection patterns. In contrast, complex networks, which are composed of nodes (individuals) and edges (connections between individuals), provide a framework for this heterogeneity, enabling more accurate modeling of such phenomena [8].
In fact, the pioneering research presented by Pastor and Vespignani in [30, 32, 31] on epidemic spreading in scale-free networks constituted an important step in the development of epidemic models on complex networks. Through their study of an SIS epidemic model using a mean-field approximation [30], they showed that the decentralized nature of scale-free networks allows infections to spread and persist easily, and that the epidemic threshold λ_c approaches zero as the network size increases, which means that even infection with a very low effective spreading becomes endemic. However, the definitive mathematical proof of the global stability in this model was established later in [40, 7].
Recently, the global dynamics of epidemic models on complex networks have been investigated by many researchers [41, 45, 22, 48, 26, 24, 6, 9, 27, 1]. In [24], Li and Zhu applied the Lyapunov functions method to examine the global stability of an SIQS model with a bilinear incidence rate. Subsequently, in [6], Xinxin and Yi extended the investigation to the same model but with a non-monotone incidence rate. In another related study, Li and Tsai [22] focused on an SIRS model with demographic effects, where they analyzed its long-term behavior under some conditions that ensure the global stability of the equilibria. Later, in [27], the model was further generalized to incorporate a nonlinear incidence rate.

Another important factor considered in epidemic models on complex networks is time delay, which accounts for realistic phenomena such as incubation periods [34] and behavioral responses [17]. In [48], Yang and Wang proposed a modified SEIR model incorporating a time delay, where they showed that it has a strong influence on the dynamic of the system. In addition, other studies have suggested epidemic models with this factor [28, 15, 39].
To date, research on the global dynamics of multiple-strain models on complex networks remains limited, primarily due to the complexity involved in analyzing such models. However, there is significant progress in this direction [23, 42, 46]. Based on the existing literature, no studies have investigated the combined impact of time delay and saturation on the analysis of these models within complex networks. To bridge this gap, we introduce an original epidemic model that involves two competing strains on complex networks. In addition, this model integrates both time delays and saturated incidence functions.
The main contributions of this work are threefold. First, we describe realistic interactions among individuals in a population where two competing infectious strains spread under saturation effects and incubation delays. Moreover, we quantify the impact of network heterogeneity on the epidemic threshold by deriving the basic and invasion reproduction numbers, which explicitly depend on the degree heterogeneity factor. Finally, we analyze the global dynamical behavior of the proposed model and establish the stability of its equilibria.
The remainder of this paper is organized as follows: Section 2 presents the model formulation and establishes its well-posedness. It also examines the existence of equilibria and derives the conditions under which they exist. Section 3 is dedicated to analyzing the global stability of equilibria using suitable Lyapunov functionals. Section 4 is devoted to numerical simulations that illustrate and support theoretical results. Finally, Section 5 concludes the study with final remarks.

2. Dynamical model

2.1. **Mathematical model.** Recently, Kuddus et al. [19] proposed a two-strain epidemic model incorporating two nonlinear incidence rates. In this model, the population is divided into four compartments: susceptible individuals (S), individuals infected with strain 1 (I_1), individuals infected with strain 2 (I_2), and recovered individuals (R). The model is given by

$$\begin{cases} \dfrac{dS}{dt} &= \Lambda - \dfrac{\beta_1 I_1 S}{1+\alpha_1 I_1} - \dfrac{\beta_2 I_2 S}{1+\alpha_2 I_2} - \mu S, \\ \dfrac{dI_1}{dt} &= \dfrac{\beta_1 I_1 S}{1+\alpha_1 I_1} - (\omega_1 + \phi_1 + \mu) I_1, \\ \dfrac{dI_2}{dt} &= \dfrac{\beta_2 I_2 S}{1+\alpha_2 I_1} - (\omega_2 + \phi_2 + \mu) I_2, \\ \dfrac{dR}{dt} &= \omega_1 I_1 + \omega_2 I_2 - \mu R. \end{cases} \tag{2.1}$$

Here, Λ denote the recruitment rate, μ the natural mortality rate, β_i the transmission rate associated with strain i, ϕ_i the disease-induced death rate for strain i, α_i the saturation effect for strain i, and ω_i the recovery rate for strain i, for $i = 1, 2$. The model assumes a homogeneous population, in which all individuals have the same probability of acquiring the infection.

To incorporate contact heterogeneity, the population is subsequently represented as a social network, where each node corresponds to an individual, and each edge represents a potential contact between two individuals. Consequently, the population is divided into n degree classes, with $k-th$ class consisting of individuals having degree k, where n denotes the maximum degree. We denote by n the maximal degree. Let $S_k(t), I_{1,k}(t), I_{2,k}(t)$ and $R_k(t)$ represent the densities of susceptible, infected with strain 1, infected with strain 2, and recovered individuals, respectively, in the degree class k. Motivated by the work in [19], we introduce a delayed two-strain epidemic model on complex networks with two nonlinear incidence rates, composed of $4n$ equations formulated as follows:

$$\begin{cases} \dfrac{dS_k(t)}{dt} &= \Lambda - \dfrac{k\beta_1 \Theta_1(t) S_k(t)}{1+\alpha_1 \Theta_1(t)} - \dfrac{k\beta_2 \Theta_2(t) S_k(t)}{1+\alpha_2 \Theta_2(t)} - \mu S_k(t), \\ \dfrac{dI_{1,k}(t)}{dt} &= \dfrac{k\beta_1 \Theta_1(t-\tau_1) S_k(t-\tau_1)}{1+\alpha_1 \Theta_1(t-\tau_1)} e^{-\mu\tau_1} - (\omega_1 + \phi_1 + \mu) I_{1,k}(t), \\ \dfrac{dI_{2,k}(t)}{dt} &= \dfrac{k\beta_2 \Theta_2(t-\tau_2) S_k(t-\tau_2)}{1+\alpha_2 \Theta_2(t-\tau_2)} e^{-\mu\tau_2} - (\omega_2 + \phi_2 + \mu) I_{2,k}(t), \\ \dfrac{dR_k(t)}{dt} &= \omega_1 I_{1,k}(t) + \omega_2 I_{2,k}(t) - \mu R_k(t). \end{cases} \tag{2.2}$$

Here, $\Theta_1(t)$ and $\Theta_2(t)$ represent the probabilities that a randomly chosen link in the network leads to an individual infected with strain 1 and strain 2, respectively. Mathematically, they are given by

$$\Theta_1(t) = \sum_{h=1}^{n} P(h/k) I_{1,h}(t) \quad and \quad \Theta_2(t) = \sum_{h=1}^{n} P(h/k) I_{2,h}(t), \tag{2.3}$$

where $P(h/k)$ is the conditional probability that a node of degree k is connected to a node of degree h. For an uncorrelated network, $P(h/k)$ is given by $hP(h)/\langle k\rangle$, where $P(h)$ is the degree distribution and $\langle k\rangle = \sum_{h=1}^{n} hP(h)$ is the average degree of the network [30]. Consequently, $\Theta_1(t)$ and $\Theta_2(t)$ are expressed as

$$\Theta_1(t) = \frac{\sum_{h=1}^{n} hP(h)I_{1,h}}{\langle k\rangle} \quad and \quad \Theta_2(t) = \frac{\sum_{h=1}^{n} hP(h)I_{2,h}}{\langle k\rangle}. \tag{2.4}$$

To account for the incubation periods of the two infectious strains, we introduce two time delays, τ_1 and τ_2. The exponential terms $e^{-\mu\tau_1}$ and $e^{-\mu\tau_2}$ represent the survival probability of individuals infected with strains 1 and 2 during these time delays.
Since the equation for R_k is decoupled from the other equations in system (2.2), we restrict our analysis to the following reduced system:

$$\begin{cases} \dfrac{dS_k}{dt} &= \Lambda - kf_1(\Theta_1(t))S_k(t) - kf_2(\Theta_2(t))S_k(t) - \mu S_k(t), \\ \dfrac{dI_{1,k}}{dt} &= kf_1(\Theta_1(t-\tau_1))S_k(t-\tau_1)e^{-\mu\tau_1} - \chi_1 I_{1,k}(t), \\ \dfrac{dI_{2,k}}{dt} &= kf_2(\Theta_2(t-\tau_2))S_k(t-\tau_2)e^{-\mu\tau_2} - \chi_2 I_{2,k}(t), \qquad k = 1, 2, ..., n, \end{cases} \tag{2.5}$$

where $f_1(\Theta_1) = \dfrac{\beta_1\Theta_1}{1+\alpha_1\Theta_1}$, $f_2(\Theta_2) = \dfrac{\beta_2\Theta_2}{1+\alpha_2\Theta_2}$, $\chi_1 = \omega_1 + \phi_1 + \mu$, and $\chi_2 = \omega_2 + \phi_2 + \mu$.

Lemma 2.1. Let $(S_k(t), I_{1,k}(t), I_{2,k}(t))$ be a solution to (2.5). Hence, we have

$$\dot{\Theta}_1(t) = \frac{\beta_1 e^{-\mu\tau_1}\Theta_1(t-\tau_1)}{\langle k\rangle(1+\alpha_1\Theta(t-\tau_1))}\sum_{h=1}^{n} h^2P(h)S_h(t-\tau_1) - \chi_1\Theta_1(t), \tag{2.6}$$

$$\dot{\Theta}_2(t) = \frac{\beta_2 e^{-\mu\tau_2}\Theta_2(t-\tau_2)}{\langle k\rangle(1+\alpha_2\Theta(t-\tau_2))}\sum_{h=1}^{n} h^2P(h)S_h(t-\tau_2) - \chi_2\Theta_2(t). \tag{2.7}$$

Let $\tau = max\{\tau_1, \tau_2\}$. The system (2.5) is supplemented with the initial conditions:

$$S_k(\theta) = \xi_{k,1}(\theta), I_{1,k}(\theta) = \xi_{k,2}(\theta), I_{2,k}(\theta) = \xi_{k,3}(\theta), \quad \theta \in [-\tau, 0], k = 1, 2, ..., n, \tag{2.8}$$

where $\xi_k = (\xi_{k,1}, \xi_{k,2}, \xi_{k,3}) \in \mathcal{C} = C([-\tau, 0], \mathbb{R}^{3n}_+)$, $\xi_{k,i}(0) > 0$, $i = 1, 2, 3,$. Here, $\mathcal{C}$ is the Banach space of continuous functions mapping $[-\tau, 0]$ into $\mathbb{R}^{3n}_+$, equipped with the uniform norm $\|.\|_\infty$.

Lemma 2.2. Let $(S_k(t), I_{1,k}(t), I_{2,k}(t))$ be a solution of model (2.2) subject to initial conditions (2.8). Thus, for all $t > 0$ and for each $k = 1, 2, \ldots, n$, $S_k(t)$, $I_{1,k}(t)$, $I_{2,k}(t)$ remain non-negative and bounded.

Proof. We begin by proving that $S_k(t) > 0$ for all $t > 0$. Since $S_k(0) > 0$, the S_k-equation in model (2.2) together with the continuity of $S_k(t)$ ensures the existence of a sufficiently small $\rho > 0$ such that $S_k(t) > 0$ for every $t \in (0, \rho)$. Assume now,

for the sake of contradiction, that $S_k(t)$ becomes zero at some time. Then there exists $t_0 \geq \rho$ such that $S_k(t_0) = 0$, while $S_k(t) > 0$ for all $t \in (0, t_0)$. Evaluating the S_k-equation at $t = t_0$ yields $\dot{S}_k(t_0) = \Lambda$, which implies that $S_k(t)$ takes negative values for some $t < t_0$, contradicting the assumption that it remained positive on $(0, t_0)$. Hence, $S_k(t) > 0$ for all $t > 0$.
Next, we establish the non-negativity of $\Theta_1(t)$ and $\Theta_2(t)$ for all $t > 0$. Obviously, if $I_{1,k}(\theta) \geq 0$ and $I_{2,k}(\theta) \geq 0$, then we have $\Theta_1(\theta) \geq 0$ and $\Theta_2(\theta) \geq 0$ for all $\theta \in [-\tau, 0]$. To extend this result for all $t > 0$, we employ mathematical induction. Initially, we show that $\Theta_1(t)$ and $\Theta_2(t)$ remain non-negative on the interval $[0, \tau]$. Let $t \in [0, \tau]$, we have

$$\Theta_1(t-\tau_1) = \frac{\sum_{h=1}^{n} hP(h)\xi_{h,2}(t-\tau_1)}{\langle k \rangle} \geq 0 \quad \text{and} \quad \Theta_2(t-\tau_2) = \frac{\sum_{h=1}^{n} hP(h)\xi_{h,2}(t-\tau_2)}{\langle k \rangle} \geq 0.$$

Then and by applying the integrating factor method to (2.6)and (2.7), we obtain

$$e^{\chi_1 t}\Theta_1(t) = \int_0^t e^{\chi_1 s} \frac{\beta_1 e^{-\mu\tau_1}\Theta_1(s-\tau_1)}{\langle k \rangle(1+\alpha_1\Theta(s-\tau_1))} \sum_{h=1}^{n} h^2 P(h) S_h(s-\tau_1)\, ds \geq 0,$$

$$e^{\chi_2 t}\Theta_2(t) = \int_0^t e^{\chi_2 s} \frac{\beta_2 e^{-\mu\tau_2}\Theta_2(s-\tau_2)}{\langle k \rangle(1+\alpha_2\Theta(s-\tau_2))} \sum_{h=1}^{n} h^2 P(h) S_h(s-\tau_2)\, ds \geq 0.$$

Hence, we conclude that $\Theta_1(t) \geq 0$ and $\Theta_2(t) \geq 0$ for all $t \in [0, \tau]$. Applying induction on the successive intervals $[n\tau, (n+1)\tau]$, with $n \in \mathbb{N}$ allows us to conclude that $\Theta_1(t)$ and $\Theta_2(t)$ remain non-negative for all $t > 0$. In a similar way, by relying on the non-negativity of $S_k(t), \Theta_1(t), \Theta_2(t)$, one can establish that $I_k(t) \geq 0$ and $I_{2,k}(t) \geq 0$ for all $t > 0$.
Define

$$H_k(t) = S_k(t) + e^{\mu\tau_1} I_{1,k}(t+\tau_1) + e^{\mu\tau_2} I_{2,k}(t+\tau_2), \quad k = 1, 2, \ldots, n,$$

then

$$\begin{aligned} \dot{H}_k(t) &= \Lambda - \mu S_k(t) - e^{\mu\tau_1}\chi_1 I_{1,k}(t+\tau_1) - e^{\mu\tau_2}\chi_2 I_{2,k}(t+\tau_2) \\ &\leq \Lambda - \mu H_k(t), \quad k = 1, 2, \ldots, n. \end{aligned}$$

Thus

$$H_k(t) \leq H_k(0)e^{-\mu t} + \frac{\Lambda}{\mu}, \quad k = 1, 2, \ldots, n.$$

which implies that

$$\limsup_{t \to +\infty} H_k(t) \leq \frac{\Lambda}{\mu}, \quad k = 1, 2, \ldots, n.$$

Therefore, every solution of system (2.2) is bounded for all $t > 0$. □

In what follows, we suppose $\Lambda = \mu$, and study the dynamic of model (2.2) in the positive region

$$\Gamma = \{(S_k, I_{1,k}, I_{2,k} \in \mathbb{R}_+^{3n} : H_k \leq \frac{\Lambda}{\mu}, k = 1, 2, \ldots, n\}.$$

2.2. **Model equilibrium points.** By setting the derivatives of model (2.5) to zero, we obtain the following expressions:

$$S_k = \frac{\Lambda}{\mu + kf_1(\Theta_1) + kf_2(\Theta_2)}, \tag{2.9}$$

$$I_{1,k} = \frac{\Lambda k e^{-\mu\tau_1} f_1(\Theta_1)}{\chi_1(\mu + kf_1(\Theta_1) + kf_2(\Theta_2))}, \tag{2.10}$$

$$I_{2,k} = \frac{\Lambda k e^{-\mu\tau_2} f_2(\Theta_2)}{\chi_2(\mu + kf_1(\Theta_1) + kf_2(\Theta_2))}. \tag{2.11}$$

Substituting relations $I_{1,k}$ and $I_{2,k}$ into (2.4), we get

$$\begin{aligned} \Theta_1 &= \frac{\Lambda e^{-\mu\tau_1}\Theta_1}{\chi_1\langle k\rangle} \sum_{h=1}^{n} \frac{h^2 P(h)\tilde{f}_1(\Theta_1)}{\mu + hf_1(\Theta_1) + hf_2(\Theta_2)}, \\ \Theta_2 &= \frac{\Lambda e^{-\mu\tau_2}\Theta_2}{\chi_2\langle k\rangle} \sum_{h=1}^{n} \frac{h^2 P(h)\tilde{f}_2(\Theta_2)}{\mu + hf_1(\Theta_1) + hf_2(\Theta_2)}, \end{aligned} \tag{2.12}$$

where $f_1(\Theta_1) = \Theta_1\tilde{f}_1(\Theta_1)$ and $f_2(\Theta_2) = \Theta_2\tilde{f}_2(\Theta_2)$. After that, we define

$$\varphi_1(\Theta_1, \Theta_2) = \frac{\Lambda e^{-\mu\tau_1}}{\chi_1\langle k\rangle} \sum_{h=1}^{n} \frac{h^2 P(h)\tilde{f}_1(\Theta_1)}{\mu + hf_1(\Theta_1) + hf_2(\Theta_2)} - 1, \tag{2.13}$$

$$\varphi_2(\Theta_1, \Theta_2) = \frac{\Lambda e^{-\mu\tau_2}}{\chi_2\langle k\rangle} \sum_{h=1}^{n} \frac{h^2 P(h)\tilde{f}_2(\Theta_2)}{\mu + hf_1(\Theta_1) + hf_2(\Theta_2)} - 1. \tag{2.14}$$

Solving (2.12) is equivalent to solving

$$\Theta_1\varphi_1(\Theta_1, \Theta_2) = 0 \quad \textit{and} \quad \Theta_2\varphi_2(\Theta_1, \Theta_2) = 0. \tag{2.15}$$

Thus, finding the solutions to (2.15) involves identifying the equilibrium points of our model.

(1) One solution to this system is $(\Theta_1, \Theta_2) = (0, 0)$, which implies that $I_{1,k} = 0$ and $I_{2,k} = 0$, for all $k = 1, 2, \ldots, n$. This corresponds to the disease-free equilibrium

$$E_0 = (\underbrace{\Lambda/\mu,\ \Lambda/\mu,\ \ldots,\ \Lambda/\mu}_{n \text{ time}},\ \underbrace{0,\ 0,\ \ldots,\ 0}_{n \text{ time}},\ \underbrace{0,\ 0,\ \ldots,\ 0}_{n \text{ time}}).$$

(2) To determine the strain-1 endemic equilibrium, denoted by

$$E_1 = (\overline{S}_1, \overline{S}_2, \ldots, \overline{S}_n, \overline{I}_{1,1}, \overline{I}_{1,2}, \ldots, \overline{I}_{1,n}, \underbrace{0, 0, \ldots, 0}_{n \text{ time}}),$$

we seek a solution (Θ_1, Θ_2) of system (2.12), with $\Theta_1 > 0$ and $\Theta_2 = 0$. This requires finding a positive solution to $\varphi_1(\Theta_1, 0) = 0$. From (2.13), we obtain

$$\varphi_1(\Theta_1, 0) = \frac{\Lambda e^{-\mu\tau_1}}{\chi_1\langle k\rangle} \sum_{h=1}^{n} \frac{h^2 P(h)\tilde{f}_1(\Theta_1)}{\mu + hf_1(\Theta_1)} - 1 = 0.$$

Given that

$$\begin{aligned}\varphi_1(1,0) &= \frac{\Lambda e^{-\mu\tau_1}}{\chi_1\langle k\rangle}\sum_{h=1}^{n}\frac{h^2P(h)\tilde{f}_1(1)}{\mu+hf_1(1)} - 1\\ &= \frac{\Lambda e^{-\mu\tau_1}}{\chi_1\langle k\rangle}\sum_{h=1}^{n}\frac{h^2P(h)f_1(1)}{\mu+hf_1(1)} - 1\\ &< \frac{\Lambda e^{-\mu\tau_1}}{\chi_1\langle k\rangle}\sum_{h=1}^{n}\frac{h^2P(h)f_1(1)}{hf_1(1)} - 1 = \frac{\Lambda e^{-\mu\tau_1}}{\chi_1} - 1 \leq 0,\end{aligned}$$

and since $\tilde{f}_1'(\Theta_1) < 0$ and $f_1'(\Theta_1) > 0$, then

$$\frac{\partial\varphi_1(\Theta_1,0)}{\partial\Theta_1} = \frac{\Lambda e^{-\mu\tau_1}}{\chi_1\langle k\rangle}\sum_{h=1}^{n}\frac{h^2P(h)[\tilde{f}_1'(\Theta_1)(\mu+hf_1(\Theta_1)) - h\tilde{f}_1(\Theta_1)f_1'(\Theta_1)]}{(\mu+hf_1(\Theta_1))^2} < 0.$$

If

$$\varphi_1(0,0) = \frac{\Lambda e^{-\mu\tau_1}}{\chi_1\langle k\rangle}\sum_{h=1}^{n}\frac{h^2P(h)}{\mu} - 1 > 0,$$

which can be rewritten as

$$\mathcal{R}_1 := \frac{\Lambda\beta_1 e^{-\mu\tau_1}}{\chi_1\mu}\frac{\langle k^2\rangle}{\langle k\rangle} > 1,$$

where $\langle k^2\rangle = \sum_{h=1}^{n} h^2P(h)$ denote the average of the squared degrees of the network.
Then, we ensure the existence of a unique $\overline{\Theta}_1 \in (0,1)$
such that $\varphi_1(\overline{\Theta}_1, 0) = 0$.
We substitute $\Theta_1 = \overline{\Theta}_1$ and $\Theta_2 = 0$ into relations (2.9), (2.10) and (2.11). This indicates that a unique strain-1 endemic equilibrium E_1 exists if and only if $\mathcal{R}_1 > 1$.

(3) Employing the same approach as described in the preceding case, we can deduce the existence of a unique strain-2 endemic equilibrium

$$E_2 = (\widehat{S}_1, \widehat{S}_2, \ldots, \widehat{S}_n, \underbrace{0, 0, \ldots, 0}_{n \text{ time}}, \widehat{I}_{2,1}, \widehat{I}_{2,2}, \ldots, \widehat{I}_{2,n})$$

if and only if

$$\mathcal{R}_2 := \frac{\Lambda\beta_2 e^{-\mu\tau_2}}{\chi_2\mu}\frac{\langle k^2\rangle}{\langle k\rangle} > 1.$$

To interpret the biological significance of $\mathcal{R}_i$ for $i = 1, 2$, observe that only susceptible individuals can be infected with strain i, Λ/μ reflect the long-term density of susceptible individuals in the absence of infection, $1/\chi_i$ represents the average infectious period of individuals infected with strain i, $e^{-\mu\tau_i}$ is the probability that an individual infected with strain i survives during the latency period τ_i, β_i is the transmission rate of strain i and the ratio $\langle k^2\rangle/\langle k\rangle$ is an indicator of network heterogeneity: the larger of this value, the more the network contains highly

connected nodes (hubs), which can significantly enhance disease transmission. Therefore, $\mathcal{R}_i$ is defined as the basic reproduction number for strain i.

Remark 2.3. The basic reproduction number $\mathcal{R}_i$ for $i = 1, 2$ does not include the saturation parameter α_i. This is because $\mathcal{R}_i$ is calculated for the fully susceptible population at the early stage of the epidemic, where the saturation effect is negligible ($I_{i,k} \approx 0, k = 1, 2, \ldots, n$).

We now investigate the existence of a coexistence equilibrium, denoted by

$$E^* = (S_1^*, S_2^*, \ldots, S_n^*, I_{1,1}^*, I_{1,2}^*, \ldots, I_{1,n}^*, I_{2,1}^*, I_{2,2}^*, \ldots, I_{2,n}^*).$$

Assuming that $\mathcal{R}_1 > 1$ and $\mathcal{R}_2 > 1$, we introduce two threshold parameters, denoted by $\mathcal{R}_1^2$ and $\mathcal{R}_2^1$, which are defined as follows

$$\mathcal{R}_1^2 := \frac{\beta_1 e^{-\mu\tau_1}}{\chi_1\langle k\rangle}\sum_{h=1}^{n} h^2 P(h)\widehat{S}_h \quad \text{and} \quad \mathcal{R}_2^1 := \frac{\beta_2 e^{-\mu\tau_2}}{\chi_2\langle k\rangle}\sum_{h=1}^{n} h^2 P(h)\overline{S}_h.$$

$\mathcal{R}_1^2$ and $\mathcal{R}_2^1$ represent the invasion reproduction numbers of strain 1 and strain 2, respectively, they quantify the ability of one strain to invade when the other is already at its equilibrium. In particular, $\mathcal{R}_1^2 < 1$ implies that strain 1 is unable to invade the endemic state of strain 2, whereas $\mathcal{R}_2^1 < 1$ indicates that strain 2 is unable to invade the endemic state of strain 1. $\mathcal{R}_1^2$ can be computed using the same approach as for the basic reproduction number, but evaluated at the endemic state of strain 2, $\mathcal{R}_2^1$ is obtained in the same manner, except that the evaluation is performed at the endemic state of strain 1.
Intuitively, if one of these numbers is less than one, the corresponding strain cannot grow in the presence of the other strain at equilibrium, which implies that the other invasion number must be greater than 1. We demonstrate this intuition in the following lemma.

Lemma 2.4. Assume that $min\{\mathcal{R}_1, \mathcal{R}_2\} > 1$.

(1) If $\mathcal{R}_1^2 < 1$, then $\mathcal{R}_2^1 > 1$,
(2) If $\mathcal{R}_2^1 < 1$, then $\mathcal{R}_1^2 > 1$.

Proof. We prove the first assertion, while the second can be derived using the same argument.

(1) Given that $\varphi_1(\overline{\Theta}_1, 0) = 0$, we derive

$$\frac{\Lambda e^{-\mu\tau_1}\tilde{f}_1(\overline{\Theta}_1)}{\chi_1\langle k\rangle}\sum_{h=1}^{n}\frac{h^2 P(h)}{\mu + hf_1(\overline{\Theta}_1)} = 1 \Longleftrightarrow \frac{e^{-\mu\tau_1}\tilde{f}_1(\overline{\Theta}_1)}{\chi_1\langle k\rangle}\sum_{h=1}^{n} h^2 P(h)\overline{S}_h = 1,$$

with $\overline{S}_h = \dfrac{\Lambda}{\mu + hf_1(\overline{\Theta}_1)}$ for all $h = 1, 2, \ldots, n$. If

$$\mathcal{R}_1^2 = \frac{\beta_1 e^{-\mu\tau_1}}{\chi_1\langle k\rangle}\sum_{h=1}^{n} h^2 P(h)\widehat{S}_h < 1 = \frac{e^{-\mu\tau_1}\tilde{f}_1(\overline{\Theta}_1)}{\chi_1\langle k\rangle}\sum_{h=1}^{n} h^2 P(h)\overline{S}_h,$$

and since $\tilde{f}_1(\overline{\Theta}_1) < \beta_1$, it follows that $\widehat{S}_h < \overline{S}_h$ for all $h = 1, 2, 3, ..., n$. Hence

$$\mathcal{R}_2^1 = \frac{\beta_2 e^{-\mu\tau_2}}{\chi_2\langle k\rangle}\sum_{h=1}^{n} h^2 P(h)\overline{S}_h > \frac{\beta_2 e^{-\mu\tau_2}}{\chi_2\langle k\rangle}\sum_{h=1}^{n} h^2 P(h)\widehat{S}_h.$$

From $\varphi_2(0, \widehat{\Theta}_2) = 0$, we conclude that

$$\frac{\Lambda e^{-\mu\tau_2}\tilde{f}_2(\widehat{\Theta}_2)}{\chi_2\langle k\rangle}\sum_{h=1}^{n}\frac{h^2 P(h)}{\mu + h f_2(\widehat{\Theta}_2)} = 1 \Longleftrightarrow \frac{e^{-\mu\tau_2}\tilde{f}_2(\widehat{\Theta}_2)}{\chi_2\langle k\rangle}\sum_{h=1}^{n} h^2 P(h)\widehat{S}_h = 1.$$

Moreover, we can see that $\beta_2 > \tilde{f}_2(\widehat{\Theta}_2)$. Then

$$\mathcal{R}_2^1 > \frac{\beta_2 e^{-\mu\tau_2}}{\chi_2\langle k\rangle}\sum_{h=1}^{n} h^2 P(h)\widehat{S}_h > \frac{e^{-\mu\tau_2}\tilde{f}_2(\widehat{\Theta}_2)}{\chi_2\langle k\rangle}\sum_{h=1}^{n} h^2 P(h)\widehat{S}_h = 1.$$

Therefore, the proof is complete.

□

Building on the above analysis and following the idea of [46], we establish a theorem that provides sufficient conditions for the existence of a coexistence equilibrium E^*. This equilibrium represents a state in which both strains persist within the population. To achieve this, we must find a pair solution (Θ_1, Θ_2) with $\Theta_1 > 0$ and $\Theta_2 > 0$ of (2.12), or equivalently, find a positive solution of (2.15). In view of the previous result, $\mathcal{R}_1 > 1$ and $\mathcal{R}_2 > 1$ imply the existence of $\overline{\Theta}_1 \in (0, 1)$ and $\widehat{\Theta}_2 \in (0, 1)$ such that $\varphi_1(\overline{\Theta}_1, 0) = 0$ and $\varphi_2(0, \widehat{\Theta}_2) = 0$.

Theorem 2.5. *If one of the following conditions is met, then a coexistence equilibrium of (2.5) exists.*

(1) *If* $\varphi_1(0, 1) < 0$, $\varphi_2(1, 0) < 0$, $\mathcal{R}_1^2 > 1$, *and* $\mathcal{R}_2^1 > 1$.
(2) *If* $\varphi_1(0, 1) < 0$, $\varphi_2(1, 0) > 0$, *and* $\mathcal{R}_1^2 > 1$.
(3) *If* $\varphi_1(0, 1) > 0$, $\varphi_2(1, 0) < 0$, *and* $\mathcal{R}_2^1 > 1$.

Proof. Firstly and with simple calculations, we can check that

$$\frac{\partial\varphi_i(\Theta_1, \Theta_2)}{\partial\Theta_j} < 0, \quad \text{with} \quad i = 1, 2 \quad \text{and} \quad j = 1, 2.$$

Then, the intermediate value theorem ensures that there exists a curve $\varphi_1(\Theta_1, \Theta_2) = 0$ in the $\Theta_1 - \Theta_2$ plane if $\varphi_1(0, 1) > 0$ (the dashed green line in Fig.1 (left)), or $\varphi_1(0, 1) < 0$ (the solid green line shown in Figure 1(left)). Analogously, we obtain a curve $\varphi_2(\Theta_1, \Theta_2) = 0$ if $\varphi_2(1, 0) > 0$ (the dashed yellow line in Figure 2(right)), or $\varphi_2(1, 0) < 0$ (the solid yellow line in Figure2(right)).
Observe that E^* corresponds to the intersection point of the two curves $\varphi_1(\Theta_1, \Theta_2) = 0$ and $\varphi_2(\Theta_1, \Theta_2) = 0$.

(1) If $\varphi_1(0, 1) < 0$, $\varphi_2(1, 0) < 0$. Thus, there exist $\tilde{\Theta}_1 \in (0, 1)$ and $\tilde{\Theta}_2 \in (0, 1)$ such that $\varphi_1(0, \tilde{\Theta}_2) = 0$ and $\varphi_2(\tilde{\Theta}_1, 0) = 0$. The intersection of $\varphi_1(\Theta_1, \Theta_2) = 0$ and $\varphi_2(\Theta_1, \Theta_2) = 0$ occurs in two subcases: (i) $\varphi_1(0, \widehat{\Theta}_2) < 0$ and $\varphi_2(\overline{\Theta}_1, 0) < 0$ ((a) in Figure 2) ; (ii) $\varphi_1(0, \widehat{\Theta}_2) > 0$ and $\varphi_2(\overline{\Theta}_1, 0) > 0$

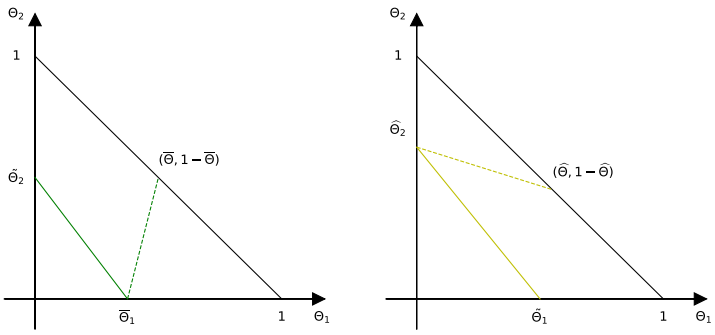


FIGURE 1. (Left): the curves $\varphi_1(\Theta_1, \Theta_2) = 0$: $\varphi_1(0,1) < 0$ (green solid curve) or $\varphi_1(0,1) > 0$ (green dashed curve). (Right): the curves $\varphi_1(\Theta_1, \Theta_2) = 0$: $\varphi_1(0,1) < 0$ (yellow solid line) or $\varphi_1(0,1) > 0$ (yellow dashed line).

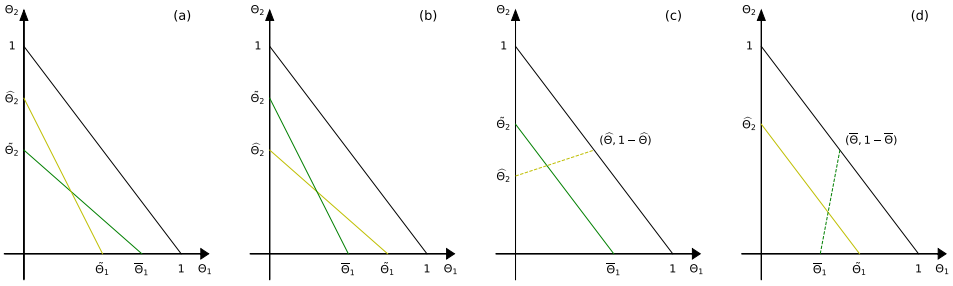


FIGURE 2. Schematic representation of four ways in which the curves $\varphi_1(\Theta_1, \Theta_2) = 0$ and $\varphi_2(\Theta_1, \Theta_2) = 0$ can intersect.

((b) in Figure 2). Next, we assert that (i) cannot occur. We have

$$\varphi_1(0, \widehat{\Theta}_2) < 0 \Longleftrightarrow \mathcal{R}_1^2 < 1 \quad \textit{and} \quad \varphi_2(\overline{\Theta}_1, 0) < 0 \Longleftrightarrow \mathcal{R}_2^1 < 1,$$

which is impossible according to Lemma 2.4 . For (ii), we readily obtain that

$$\varphi_1(0, \widehat{\Theta}_2) > 0 \Longleftrightarrow \mathcal{R}_1^2 > 1 \quad \textit{and} \quad \varphi_2(\overline{\Theta}_1, 0) > 0 \Longleftrightarrow \mathcal{R}_2^1 > 1.$$

Hence, the first condition is proved.

(2) If $\varphi_1(0,1) < 0$, $\varphi_2(1,0) > 0$. Thus, there exist $\overline{\Theta}_2 \in (0,1)$ and $\widehat{\Theta} \in (0,1)$ such that $\varphi_1(0, \overline{\Theta}_2) = 0$ and $\varphi_2(\widehat{\Theta}, 1-\widehat{\Theta}) = 0$. As a result, the curves $\varphi_1(\Theta_1, \Theta_2) = 0$ and $\varphi_2(\Theta_1, \Theta_2) = 0$ intersect if $\varphi_1(0, \widehat{\Theta}_2) > 0$ ((c) in Figure 2). We have

$$\varphi_1(0, \widehat{\Theta}_2) = \frac{1}{\langle k \rangle} \sum_{h=1}^{n} h^2 P(h) \frac{\beta_1}{\chi_1} e^{-\mu \tau_1} \widehat{S}_h - 1 = \mathcal{R}_1^2 - 1 > 0 \Longleftrightarrow \mathcal{R}_1^2 > 1.$$

Hence, the second condition is proved.

(3) If $\varphi_1(0,1) > 0$, $\varphi_2(1,0) < 0$. Thus, there exist $\widehat{\Theta}_1 \in (0,1)$ and $\overline{\Theta} \in (0,1)$ such that $\varphi_1(\overline{\Theta}, 1-\overline{\Theta}) = 0$ and $\varphi_2(\widehat{\Theta}_1, 0) = 0$. As a result, the curves $\varphi_1(\Theta_1,\Theta_2) = 0$ and $\varphi_2(\Theta_1,\Theta_2) = 0$ intersect if $\varphi_2(\overline{\Theta}_1, 0) > 0$ ((d) in Figure 2). We have

$$\varphi_2(\overline{\Theta}_1, 0) = \frac{1}{\langle k\rangle}\sum_{h=1}^{n} h^2 P(h)\frac{\beta_2}{\chi_2} e^{-\mu\tau_2}\overline{S}_h - 1 = \mathcal{R}_2^1 - 1 > 0 \Longleftrightarrow \mathcal{R}_2^1 > 1.$$

Hence, the last condition is proved.

□

3. Global asymptotic stability (GAS)

This section is dedicated to analyzing the global stability of the equilibrium points using the Lyapunov functional method. We use the function $\Phi(x) = x - 1 - \ln(x)$, where $\Phi(1) = 0$ and $\Phi(x) > 0$ for all $x > 0$.
For brevity, we denote
$X = X(t)$ and $X^\tau = X(t-\tau)$ for any $X \in \{S_k, \Theta_1, \Theta_2\}$ and $\tau \in \{\tau_1, \tau_2\}$, with $k = 1, 2, ..., n$.

Theorem 3.1. *If $max\{\mathcal{R}_1, \mathcal{R}_2\} < 1$, then E_0 is GAS.*

Proof. We define the Lyapunov function $\mathcal{L}_0$ by

$$\mathcal{L}_0(t) = \frac{1}{\langle k\rangle}\sum_{h=1}^{n} hP(h)\Bigg\{ S_h^0\Phi\left(\frac{S_h}{S_h^0}\right) + \int_{t-\tau_1}^{t} hf_1(\Theta_1(u))S_h(u)\,du + \int_{t-\tau_2}^{t} hf_2(\Theta_2(u))S_h(u)\,du\Bigg\} + e^{\mu\tau_1}\Theta_1 + e^{\mu\tau_2}\Theta_2.$$

Taking the derivative of $\mathcal{L}_0(t)$ along any solution of system (2.5), it shows that

$$\dot{\mathcal{L}}_0(t) = \frac{1}{\langle k\rangle}\sum_{h=1}^{n} hP(h)\Bigg\{ \left(1 - \frac{S_h^0}{S_h}\right)\dot{S}_h + (hf_1(\Theta_1)S_h - hf_1(\Theta_1^{\tau_1})S_h^{\tau_1}) + (hf_2(\Theta_2)S_h - hf_2(\Theta_2^{\tau_2})S_h^{\tau_2})\Bigg\} + e^{\mu\tau_1}\dot{\Theta}_1 + e^{\mu\tau_2}\dot{\Theta}_2.$$

Combining system (2.5) with the expressions given in (2.6) and (2.7), and using $\Lambda = \mu S_K^0$, we obtain

$$\begin{aligned}\dot{\mathcal{L}}_0(t) &= \frac{1}{\langle k\rangle}\sum_{h=1}^{n} hP(h)\left\{\mu S_h^0 - \mu S_h - \frac{S_h^0}{S_h}\mu S_h^0 + \mu S_h^0 + hf_1(\Theta_1)S_h^0 + hf_2(\Theta_2)S_h^0\right\} \\ &\quad - e^{\mu\tau_1}\chi_1\Theta_1 - e^{\mu\tau_2}\chi_2\Theta_2 \\ &= \frac{1}{\langle k\rangle}\sum_{h=1}^{n} hP(h)\mu S_h^0\left(2 - \frac{S_h}{S_h^0} - \frac{S_h^0}{S_h}\right) + \frac{1}{\langle k\rangle}\sum_{h=1}^{n} h^2P(h)f_1(\Theta_1)S_h^0 \\ &\quad - e^{\mu\tau_1}\chi_1\Theta_1 + \frac{1}{\langle k\rangle}\sum_{h=1}^{n} h^2P(h)f_2(\Theta_2)S_h^0 - e^{\mu\tau_2}\chi_2\Theta_2.\end{aligned}$$

We can see that

$$f_1(\Theta_1) \leq \beta_1\Theta_1 \quad and \quad f_2(\Theta_2) \leq \beta_2\Theta_2,$$

and from the AM-GM inequality it follows that

$$2 - \frac{S_h}{S_h^0} - \frac{S_h^0}{S_h} \leq 0.$$

Then

$$\begin{aligned}\dot{\mathcal{L}}_0(t) \leq & \left(\frac{e^{-\mu\tau_1}}{\chi_1\langle k\rangle}\sum_{h=1}^{n} h^2P(h)\beta_1S_h^0 - 1\right)e^{\mu\tau_1}\chi_1\Theta_1 \\ & + \left(\frac{e^{-\mu\tau_2}}{\chi_2\langle k\rangle}\sum_{h=1}^{n} h^2P(h)\beta_2S_h^0 - 1\right)e^{\mu\tau_2}\chi_2\Theta_2 \\ & \leq (\mathcal{R}_1 - 1)\, e^{\mu\tau_1}\chi_1\Theta_1 + (\mathcal{R}_2 - 1)\, e^{\mu\tau_2}\chi_2\Theta_2.\end{aligned}$$

If $\mathcal{R}_1 < 1$ and $\mathcal{R}_2 < 1$, then $\dot{\mathcal{L}}_1(t) \leq 0$ and equality holds if and only if $S_h = S_h^0$, $I_{1,h} = 0$, and $I_{2,h} = 0$ for all $h = 1, 2, \ldots, n$. By LaSalle's Invariance Principle [12], we conclude that E_0 is GAS. □

Theorem 3.2. *If any of the following conditions is satisfied*
(i) $\mathcal{R}_2 < 1 < \mathcal{R}_1$.
(ii) $\mathcal{R}_1^2 > 1$ *and* $\mathcal{R}_2^1 < 1 < \mathcal{R}_2$.
Therefore, E_1 *is GAS.*

Proof. We define the Lyapunov function $\mathcal{L}_1$ by

$$\begin{aligned}\mathcal{L}_1(t) = & \frac{1}{\langle k\rangle}\sum_{h=1}^{n} hP(h)\Bigg\{\overline{S}_h\Phi\left(\frac{S_h}{\overline{S}_h}\right) + \int_{t-\tau_1}^{t} hf_1(\overline{\Theta}_1)\overline{S}_h\Phi\left(\frac{f_1(\Theta_1(u))S_h(u)}{f_1(\overline{\Theta}_1)\overline{S}_h}\right)du \\ & + \int_{t-\tau_2}^{t} hf_2(\Theta_2(u))S_h(u)\,du\Bigg\} \\ & + e^{\mu\tau_1}\left(\Theta_1 - \overline{\Theta}_1 - \int_{\overline{\Theta}_1}^{\Theta_1}\frac{f_1(\overline{\Theta}_1)}{f_1(u)}\,du\right) + e^{\mu\tau_2}\Theta_2.\end{aligned}$$

Along the solutions of system (2.5), the derivative of $\mathcal{L}_1(t)$ is given by

$$\begin{aligned}\dot{\mathcal{L}}_1(t) = & \frac{1}{\langle k\rangle}\sum_{h=1}^{n} hP(h)\Bigg\{\left(1 - \frac{\overline{S}_h}{S_h}\right)\dot{S}_h \\ & + hf_1(\overline{\Theta}_1)\overline{S}_h\left(\Phi\left(\frac{f_1(\Theta_1)S_h}{f_1(\overline{\Theta}_1)\overline{S}_h}\right) - \Phi\left(\frac{f_1(\Theta_1^{\tau_1})S_h^{\tau_1}}{f_1(\overline{\Theta}_1)\overline{S}_h}\right)\right) \\ & + (hf_2(\Theta_2)S_h - hf_2(\Theta_2^{\tau_2})S_h^{\tau_2})\Bigg\} + e^{\mu\tau_1}\left(1 - \frac{f_1(\overline{\Theta}_1)}{f_1(\Theta_1)}\right)\dot{\Theta}_1 + e^{\mu\tau_2}\dot{\Theta}_2.\end{aligned}$$

In the equilibrium point E_1, the system (2.5) verifies the following identities

$$\Lambda = \mu\overline{S}_h + hf_1(\overline{\Theta}_1)\overline{S}_h \quad and \quad \chi_1 = \frac{1}{\langle k\rangle}\sum_{h=1}^{n} h^2P(h)\frac{f_1(\overline{\Theta}_1)\overline{S}_h}{\overline{\Theta}_1}e^{-\mu\tau_1}.$$

Therefore

$$\begin{aligned}\dot{\mathcal{L}}_1(t) = \frac{1}{\langle k\rangle}\sum_{h=1}^{n} hP(h)\mu\overline{S}_h\left(2-\frac{S_h}{\overline{S}_h}-\frac{\overline{S}_h}{S_h}\right)+\frac{1}{\langle k\rangle}\sum_{h=1}^{n} h^2P(h)\Bigg\{f_1(\overline{\Theta}_1)\overline{S}_h\\ -\frac{\overline{S}_h}{S_h}f_1(\overline{\Theta}_1)\overline{S}_h+f_1(\Theta_1)\overline{S}_h+f_1(\overline{\Theta}_1)\overline{S}_h\ln\left(\frac{f_1(\Theta_1^{\tau_1})S_h^{\tau_1}}{f_1(\Theta_1)S_h}\right)\\ -f_1(\overline{\Theta}_1)\overline{S}_h\frac{\Theta_1}{\overline{\Theta}_1}-f_1(\Theta_1^{\tau_1})S_h^{\tau_1}\frac{f_1(\overline{\Theta}_1)}{f_1(\Theta_1)}\\ +f_1(\overline{\Theta}_1)\overline{S}_h\frac{f_1(\overline{\Theta}_1)}{f_1(\Theta_1)}\frac{\Theta_1}{\overline{\Theta}_1}\Bigg\}+\left(\frac{e^{\mu\tau_2}}{\chi_2\langle k\rangle}\sum_{h=1}^{n} h^2P(h)\frac{f_2(\Theta_2)}{\Theta_2}\overline{S}_h-1\right)e^{\mu\tau_2}\chi_2\Theta_2,\end{aligned}$$

we invoke the two inequalities

$$f_2(\Theta_2)\le\beta_2\Theta_2 \quad and \quad 2-\frac{S_h}{\overline{S}_h}-\frac{\overline{S}_h}{S_h}\le 0,$$

to obtain

$$\begin{aligned}\dot{\mathcal{L}}_1(t)\le\frac{1}{\langle k\rangle}\sum_{h=1}^{n} h^2P(h)\Bigg\{f_1(\overline{\Theta}_1)\Bigg(2\overline{S}_h-\overline{S}_h\frac{\overline{S}_h}{S_h}-\frac{f_1(\Theta_1^{\tau_1})S_h^{\tau_1}}{f_1(\Theta_1)}\\ -\overline{S}_h\ln\left(\frac{f_1(\Theta_1)S_h}{f_1(\Theta_1^{\tau_1})S_h^{\tau_1}}\right)\Bigg)+f_1(\Theta_1)\overline{S}_h-f_1(\overline{\Theta}_1)\overline{S}_h\frac{\Theta_1}{\overline{\Theta}_1}+f_1(\overline{\Theta}_1)\overline{S}_h\frac{f_1(\overline{\Theta}_1)}{f_1(\Theta_1)}\frac{\Theta_1}{\overline{\Theta}_1}\\ -f_1(\overline{\Theta}_1)\overline{S}_h\Bigg\}+(\mathcal{R}_2^1-1)e^{\mu\tau_2}\chi_2\Theta_2.\end{aligned}$$

Note that

$$2\overline{S}_h-\overline{S}_h\frac{\overline{S}_h}{S_h}-\frac{f_1(\Theta_1^{\tau_1})S_h^{\tau_1}}{f_1(\Theta_1)}-\overline{S}_h\ln\left(\frac{f_1(\Theta_1)S_h}{f_1(\Theta_1^{\tau_1})S_h^{\tau_1}}\right)=-\overline{S}_h\left(\Phi\left(\frac{\overline{S}_h}{S_h}\right)+\Phi\left(\frac{f_1(\Theta_1^{\tau_1})S_h^{\tau_1}}{f_1(\Theta_1)\overline{S}_h}\right)\right)\le 0.$$

Therefore

$$\begin{aligned}\dot{\mathcal{L}}_1(t)\le\frac{1}{\langle k\rangle}\sum_{h=1}^{n} h^2P(h)\Bigg\{f_1(\overline{\Theta}_1)\overline{S}_h\left(\frac{\Theta_1}{\overline{\Theta}_1}-\frac{f_1(\Theta_1)}{f_1(\overline{\Theta}_1)}\right)\left(\frac{f_1(\overline{\Theta}_1)}{f_1(\Theta_1)}-1\right)\Bigg\}\\ +(\mathcal{R}_2^1-1)e^{\mu\tau_2}\chi_2\Theta_2.\end{aligned}$$

Since f_1 is a strictly decreasing function, that is

$$\left(\frac{\Theta_1}{\overline{\Theta}_1}-\frac{f_1(\Theta_1)}{f_1(\overline{\Theta}_1)}\right)\left(\frac{f_1(\overline{\Theta}_1)}{f_1(\Theta_1)}-1\right)\le 0.$$

Therefore, $\dot{\mathcal{L}}_1(t)\le 0$ and equality holds if and only if $S_h=\overline{S}_h$, $I_{1,h}=\overline{I}_{1,h}$, and $I_{2,h}=0$ for all $h=1,2,\ldots,n$. By LaSalle's Invariance Principle [12], we conclude that E_1 is GAS. □

Theorem 3.3. *If any of the following conditions is satisfied*
(i) $\mathcal{R}_1 < 1 < \mathcal{R}_2$
(ii) $\mathcal{R}_2^1 > 1$ *and* $\mathcal{R}_1^2 < 1 < \mathcal{R}_1$.
Then, E_2 *is GAS.*

Proof. We prove this theorem similarly to Theorem 3.2. □

We now demonstrate that E^* is GAS.

Theorem 3.4. *Suppose that* E^* *exists, then it is GAS.*

Proof. Let us define the Lyapunov function

$$\begin{aligned}\mathcal{L}_3(t) =& \frac{1}{\langle k\rangle}\sum_{h=1}^{n} hP(h)\Bigg\{ S_h^*\Phi\left(\frac{S_h}{S_h^*}\right) + \int_{t-\tau_1}^{t} hf_1(\Theta_1^*)S_h^*\Phi\left(\frac{f_1(\Theta_1(u))S_h(u)}{f_1(\Theta_1^*)S_h^*}\right)du \\ &+ \int_{t-\tau_2}^{t} hf_2(\Theta_2^*)S_h^*\Phi\left(\frac{f_2(\Theta_2(u))S_h(u)}{f_2(\Theta_2^*)S_h^*}\right)du\Bigg\} \\ &+ e^{\mu\tau_1}\left(\Theta_1 - \Theta_1^* - \int_{\Theta_1^*}^{\Theta_1}\frac{f_1(\Theta_1^*)}{f_1(u)}\,du\right) \\ &+ e^{\mu\tau_2}\left(\Theta_2 - \Theta_2^* - \int_{\Theta_2^*}^{\Theta_2}\frac{f_2(\Theta_2^*)}{f_2(u)}\,du\right).\end{aligned}$$

Taking the derivative of $\mathcal{L}_3(t)$ along any solution of system (2.5), it shows that

$$\begin{aligned}\dot{\mathcal{L}}_3(t) =& \frac{1}{\langle k\rangle}\sum_{h=1}^{n} hP(h)\Bigg\{\left(1-\frac{S_h^*}{S_h}\right)\dot{S}_h + hf_1(\Theta_1^*)S_h^*\Bigg(\Phi\left(\frac{f_1(\Theta_1)S_h}{f_1(\Theta_1^*)S_h^*}\right) - \\ &\Phi\left(\frac{f_1(\Theta_1^{\tau_1})S_h^{\tau_1}}{f_1(\Theta_1^*)S_h^*}\right)\Bigg) \\ &+ hf_2(\Theta_2^*)S_h^*\left(\Phi\left(\frac{f_2(\Theta_2)S_h}{f_2(\Theta_2^*)S_h^*}\right) - \Phi\left(\frac{f_2(\Theta_2^{\tau_2})S_h^{\tau_2}}{f_2(\Theta_2^*)S_h^*}\right)\right)\Bigg\} \\ &+ e^{\mu\tau_1}\left(1-\frac{f_1(\Theta_1^*)}{f_1(\Theta_1)}\right)\dot{\Theta}_1 + e^{\mu\tau_2}\left(1-\frac{f_2(\Theta_2^*)}{f_2(\Theta_2)}\right)\dot{\Theta}_2\end{aligned}$$

In the equilibrium point E^*, the system (2.5) verifies the following relations

$$\begin{cases}\Lambda = \mu S_h^* + hf_1(\Theta_1^*)S_h^* + hf_2(\Theta_2^*)S_h^*, \\ \chi_1 = \dfrac{1}{\langle k\rangle}\displaystyle\sum_{h=1}^{n} h^2P(h)\frac{f_1(\Theta_1^*)S_h^*}{\Theta_1^*}e^{-\mu\tau_1}, \\ \chi_2 = \dfrac{1}{\langle k\rangle}\displaystyle\sum_{h=1}^{n} h^2P(h)\frac{f_2(\Theta_2^*)S_h^*}{\Theta_2^*}e^{-\mu\tau_2}.\end{cases}$$

Therefore

$$\begin{aligned}\dot{\mathcal{L}}_3(t) = &\frac{1}{\langle k\rangle}\sum_{h=1}^{n} hP(h)\mu S_h^*\left(2-\frac{S_h}{S_h^*}-\frac{S_h^*}{S_h}\right)\\
&+\frac{1}{\langle k\rangle}\sum_{h=1}^{n} h^2P(h)\Bigg\{f_1(\Theta_1^*)S_h^*-\frac{S_h^*}{S_h}f_1(\Theta_1^*)S_h^*+f_1(\Theta_1)S_h^*\\
&+f_1(\Theta_1^*)S_h^*\ln\left(\frac{f_1(\Theta_1^{\tau_1})S_h^{\tau_1}}{f_1(\Theta_1)S_h}\right)-f_1(\Theta_1^*)S_h^*\frac{\Theta_1}{\Theta_1^*}-f_1(\Theta_1^{\tau_1})S_h^{\tau_1}\frac{f_1(\Theta_1^*)}{f_1(\Theta_1)}\\
&+f_1(\Theta_1^*)S_h^*\frac{f_1(\Theta_1^*)}{f_1(\Theta_1)}\frac{\Theta_1}{\Theta_1^*}\Bigg\}+\frac{1}{\langle k\rangle}\sum_{h=1}^{n} h^2P(h)\Bigg\{f_2(\Theta_2^*)S_h^*-\frac{S_h^*}{S_h}f_2(\Theta_2^*)S_h^*\\
&+f_2(\Theta_2)S_h^*+f_2(\Theta_2^*)S_h^*\ln\left(\frac{f_2(\Theta_2^{\tau_2})S_h^{\tau_2}}{f_2(\Theta_2)S_h}\right)-f_2(\Theta_2^*)S_h^*\frac{\Theta_2}{\Theta_2^*}\\
&-f_2(\Theta_2^{\tau_2})S_h^{\tau_2}\frac{f_2(\Theta_2^*)}{f_2(\Theta_2)}+f_2(\Theta_2^*)S_h^*\frac{f_2(\Theta_2^*)}{f_2(\Theta_2)}\frac{\Theta_2}{\Theta_2^*}\Bigg\},\end{aligned}$$

We obtain, after straightforward calculations

$$\begin{aligned}\dot{\mathcal{L}}_3(t) = &\frac{1}{\langle k\rangle}\sum_{h=1}^{n} h^2P(h)\Bigg\{\mu S_h^*\left(2-\frac{S_h}{S_h^*}-\frac{S_h^*}{S_h}\right)\\
&-f_1(\Theta_1^*)S_h^*\left(\Phi\left(\frac{S_h^*}{S_h}\right)+\Phi\left(\frac{f_1(\Theta_1^{\tau_1})S_h^{\tau_1}}{f_1(\Theta_1)S_h^*}\right)\right)\\
&+f_1(\Theta_1^*)S_h^*\left(-\frac{\Theta_1}{\Theta_1^*}+\frac{f_1(\Theta_1)}{f_1(\Theta_1^*)}+\frac{f_1(\Theta_1^*)}{f_1(\Theta_1)}\frac{\Theta_1}{\Theta_1^*}-1\right)\Bigg\}\\
&+\frac{1}{\langle k\rangle}\sum_{h=1}^{n} h^2P(h)\Bigg\{-f_2(\Theta_2^*)S_h^*\left(\Phi\left(\frac{S_h^*}{S_h}\right)+\Phi\left(\frac{f_2(\Theta_2^{\tau_2})S_h^{\tau_2}}{f_2(\Theta_2)S_h^*}\right)\right)\\
&+f_2(\Theta_2^*)S_h^*\left(-\frac{\Theta_2}{\Theta_2^*}+\frac{f_2(\Theta_2)}{f_2(\Theta_2^*)}+\frac{f_2(\Theta_2^*)}{f_2(\Theta_2)}\frac{\Theta_2}{\Theta_2^*}-1\right)\Bigg\}\end{aligned}$$

By applying the same reasoning as in Theorem 3.2, we obtain $\dot{\mathcal{L}}_3(t)\leq 0$ and equality holds if and only if $S_h = S_h^*$, $I_{1,h} = I_{1,h}^*$, and $I_{2,h} = I_{2,h}^*$ for all $h = 1, 2, \ldots, n$.
By LaSalle's Invariance Principle [12], we conclude that E^* is GAS. □

4. Numerical simulations

To validate the analytical findings derived in the preceding sections, we will conduct numerical simulations of system (2.5) on a scale-free network with a power-law degree distribution given by $P(k) = \eta k^{-2.5}$. We choose η in order that $\sum_{h=1}^{100} P(h) = 1$. In this case, we obtain $\langle k\rangle = 1.7995$ and $\langle k^2\rangle = 13.8642$. The

average densities of nodes infected with strains 1 and 2 are given by

$$I_1(t) = \sum_{k=1}^{n} P(k) I_{1,k}(t) \quad \text{and} \quad I_2(t) = \sum_{k=1}^{n} P(k) I_{2,k}(t) \tag{4.1}$$

TABLE 1. Description of model parameters

Parameters	Value and unit	References
μ	0.07/365 (day^{-1})	[21]
β_1	Varied (day^{-1})	- -
β_2	Varied (day^{-1})	- -
τ_1	500 (day)	Estimated
τ_2	600 (day)	Estimated
α_1	0.015	[37]
α_2	0.015	[37]
ω_1	0.291/365 (day^{-1})	[36]
ω_2	0.145/365 (day^{-1})	[20]
ϕ_1	0.37/(3×365) (day^{-1})	[35]
ϕ_2	0.37/(3×365) (day^{-1})	[35]

4.1. **Sensitivity analysis.** Sensitivity analysis is used to determine the parameters that have the strongest or weakest impact on the model results and to identify the main factors that influence the spread of infectious diseases. In this study, we use the Partial Rank Correlation Coefficient (PRCC) combined with the Latin Hypercube Sampling (LHS) method. The model outputs considered are the basic reproduction numbers $\mathcal{R}_1$ and $\mathcal{R}_2$, along with the invasion reproduction numbers $\mathcal{R}_1^2$ and $\mathcal{R}_2^1$. As shown in Fig. 3 (left panel), $\mathcal{R}_1$ exhibits a strong positive correlation with β_1, indicating that increases in this parameter lead to higher values of $\mathcal{R}_1$. The parameters ω_1 and ϕ_1 have a strong negative correlation with $\mathcal{R}_1$, while τ_1 displays the weakest negative correlation. From Fig. 3 (right panel), $\mathcal{R}_2$ exhibits a strong positive correlation with β_2, indicating that increases in this parameter lead to higher values of $\mathcal{R}_2$. The parameters ω_2 and ϕ_2 have a strong negative correlation with $\mathcal{R}_2$, while τ_2 displays the weakest negative correlation. Fig. 4 (left panel) shows that $\mathcal{R}_1^2$ is positively correlated with β_1 and α_2, and negatively correlated with τ_1, ω_1, ϕ_1, β_2. Fig. 4 (right panel) shows that $\mathcal{R}_2^1$ is positively correlated with β_2 and α_1, and negatively correlated with τ_2, ω_2, ϕ_2, β_1.

4.2. **Stability of the equilibria.** In this subsection, we perform numerical simulations of system (2.5) to demonstrate the stability behavior of the equilibrium points discussed in Section 3. The simulations are carried out for five selected degrees $k = 25, 50, 75, 100$. For each degree, we plot the time evolution of the densities of $S_k(t)$, $I_{1,k}(t)$ and $I_{2,k}(t)$.

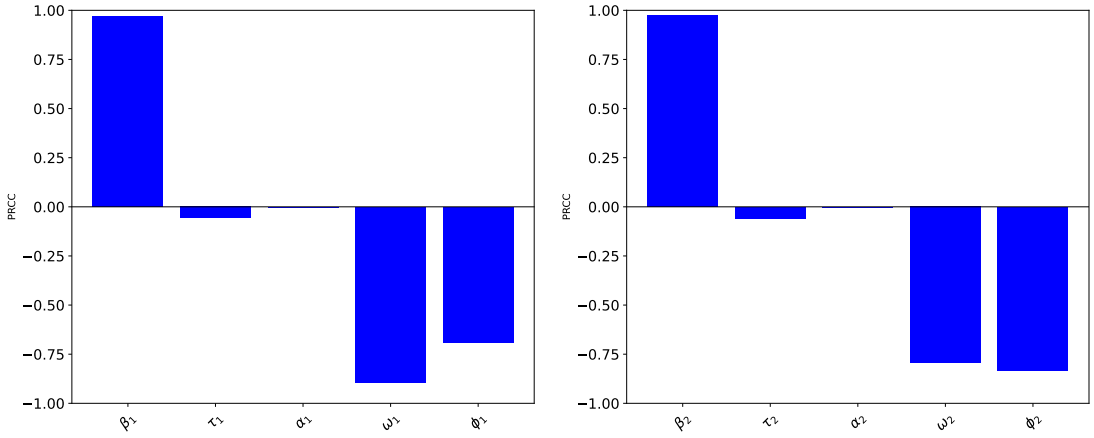


FIGURE 3. PRCC analysis of the basic reproduction number $\mathcal{R}_1$ ($\mathcal{R}_2$) with respect to model parameters β_1, τ_1, α_1, ω_1, ϕ_1 (β_2, τ_2, α_2, ω_2, ϕ_2)

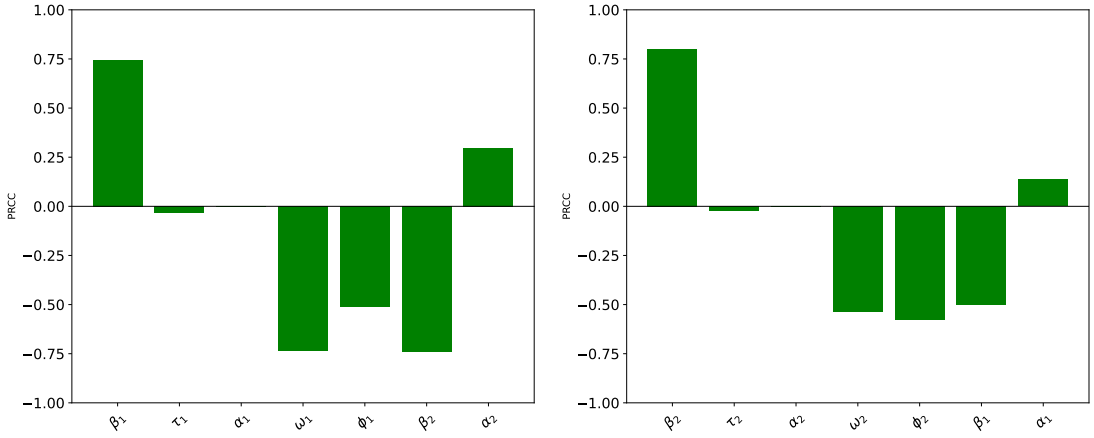


FIGURE 4. PRCC analysis of the invasion reproduction number $\mathcal{R}_1^2$ ($\mathcal{R}_2^1$) with respect to model parameters β_1, τ_1, α_1, ω_1, ϕ_1, β_2, α_2 (β_2, τ_2, α_2, ω_2, ϕ_2, β_1, α_1)

Example 4.1. We start first by examining the stability of the disease free equilibrium E_0. We set $\beta_1 = 0.00005$, $\beta_2 = 0.00004$, while the remaining parameter values are listed in Table 1, we find $\mathcal{R}_1 = 0.26 < 1$ and $\mathcal{R}_2 = 0.29 < 1$. According to Theorem 3.1, E_0 is GAS. Figure 5 illustrates that, regardless of the degree k, the densities $I_{1,k}(t)$ and $I_{2,k}$ (t) vanish over time, while $S_k(t)$ approaches Λ/μ.

Example 4.2. The stability of E_1 is verified using the value parameters: $\beta_1 = 0.0003$, $\beta_2 = 0.00014$. Thus, we find $\mathcal{R}_1 = 1.59 > 1$ and $\mathcal{R}_2 = 1.04 > 1$. After calculating $\overline{\Theta}_1 = 0.014$ and $\widehat{\Theta}_2 = 0.001$, we find $\mathcal{R}_1^2 = 1.53 > 1$ and $\mathcal{R}_2^1 = 0.65 < 1$. From Theorem 3.2 (ii), we deduce that E_1 is GAS. This conclusion is identical to the result obtained in Figure. 6.

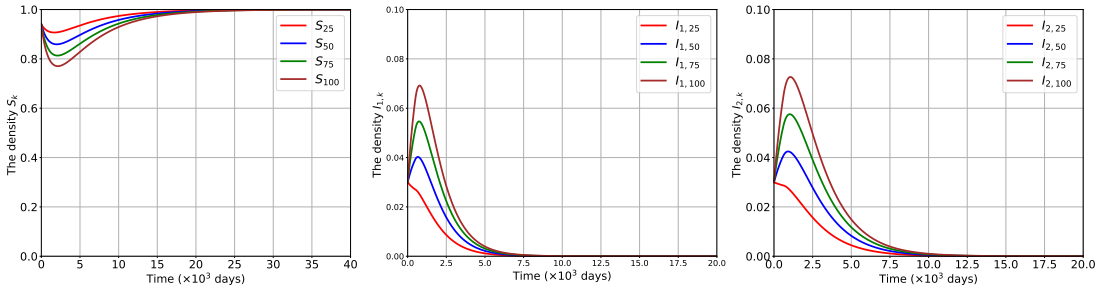


FIGURE 5. Time series plots of $S_k(t)$, $I_{1,k}(t)$ and $I_{2,k}(t)$ for $k = 25, 50, 75, 100$.

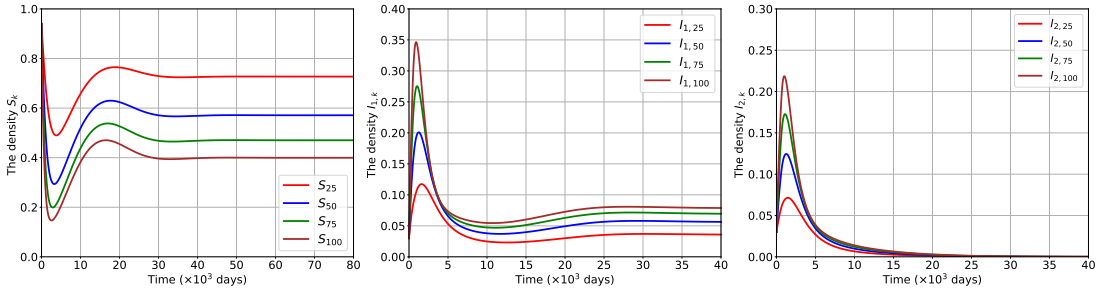


FIGURE 6. Time series plots of $S_k(t)$, $I_{1,k}(t)$ and $I_{2,k}(t)$ for $k = 25, 50, 75, 100$.

Example 4.3. Next, we examine the scenario where $\mathcal{R}_1 < 1$ and $\mathcal{R}_2 > 1$. With $\beta_1 = 0.0001$, $\beta_2 = 0.00018$, we find $\mathcal{R}_1 = 0.53 < 1$ and $\mathcal{R}_2 = 1.33 > 1$. Theorem 3.3(i) then implies that E_2 is GAS, which is confirmed in Figure 7.

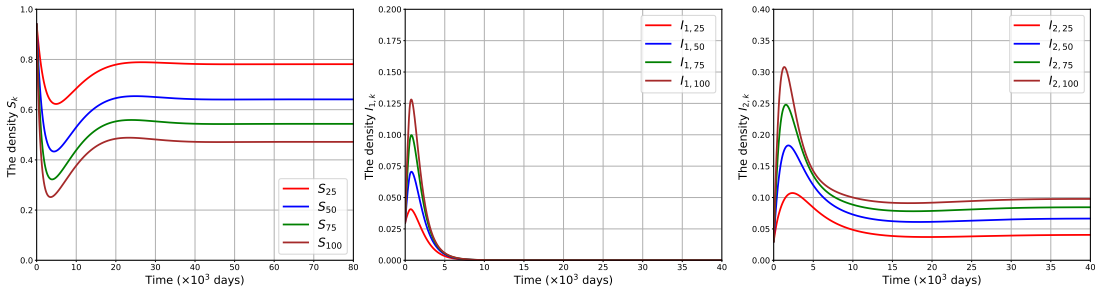


FIGURE 7. Time series plots of $S_k(t)$, $I_{1,k}(t)$ and $I_{2,k}(t)$ for $k = 25, 50, 75, 100$.

Example 4.4. In order to satisfy one of the conditions in Theorem 2.5, we chose $\beta_1 = 0.0003$ and $\beta_2 = 0.000206$. Then $\mathcal{R}_1 = 1.5557 > 1$ and $\mathcal{R}_2 = 1.5556 > 1$. After calculating $\Theta_1^* = 0.013$ and $\Theta_2^* = 0.019$, we can check that $\mathcal{R}_1^2 = 1.00034 > 1$, $\mathcal{R}_2^1 = 1.00014 > 1$, $\varphi_1(0,1) < 0$ and $\varphi_2(1,0) < 0$. According to Theorem 2.5 (first condition) and Theorem 3.4, E^* exists and is GAS, which is confirmed in Figure 8.

4.3. **The effect of the time delays τ_1 and τ_2.** Since time delays play an important role in epidemic transmission, we next investigate their impact on

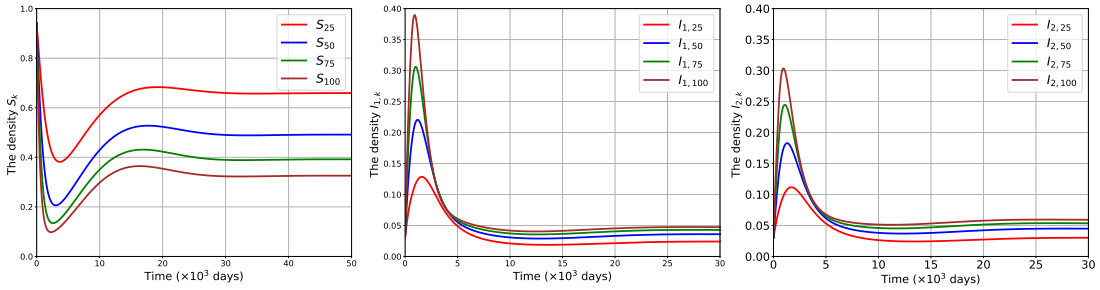


FIGURE 8. Time series plots of $S_k(t)$, $I_{1,k}(t)$ and $I_{2,k}(t)$ for $k = 25, 50, 75, 100$.

the dynamics of model (2.5). In particular, we compare the temporal evolution of $I_1(t)$ and $I_2(t)$ under two different delay scenarios: $(\tau_1, \tau_2) = (500, 600)$ and $(\tau_1, \tau_2) = (2000, 1900)$. The transmission rates are fixed at $\beta_1 = 0.0002$ and $\beta_2 = 0.0001$, while the remaining parameter values are given in Table 1.
For the first scenario, we obtain $\mathcal{R}_1 = 1.23 > 1$ and $\mathcal{R}_2 = 0.78 < 1$. According to Theorem 3.2, E_1 is GAS, indicating that strain-1 persists whereas strain-2 dies out. For the second scenario, we obtain $\mathcal{R}_1 = 0.81 < 1$ and $\mathcal{R}_2 = 0.58 < 1$. Hence, according to Theorem 3.1, the disease-free equilibrium E_0 is GAS, which implies that both strains eventually disappear. These results demonstrate that time delays can alter the long-term behavior of epidemic models by changing the stability of equilibria. Furthermore, Figure 9 shows that increasing both τ_1 and τ_2 does not necessarily suppress the transmission of both strains. This phenomenon can be attributed to the competitive interaction between the two strains.

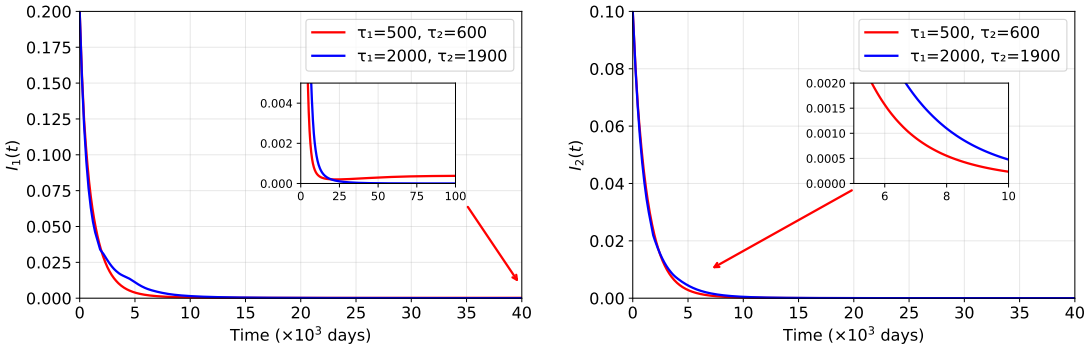


FIGURE 9. Effect of the time delays τ_1 and τ_2

5. CONCLUSION

In this work, we developed and investigated a delayed two-strain epidemic model with nonlinear saturated incidence rates on complex networks. By incorporating heterogeneous contact patterns, the proposed framework provides a more realistic description of disease transmission than traditional homogeneous mixing models. The main contributions of this study are threefold. First, we rigorously established the well-posedness of the model by proving the positivity and

boundedness of solutions. Second, we derived the basic and invasion reproduction numbers, which fully characterize the existence of all possible equilibria, including the disease-free, two boundary endemic, and coexistence equilibria. Third, by constructing appropriate Lyapunov functionals, we obtained sufficient conditions for the global asymptotic stability of each equilibrium, thereby providing a complete picture of the long-term dynamics of our model. Numerical simulations on scale-free networks not only validated the theoretical results but also highlighted the significant roles of time delays in shaping the competitive outcomes between the two strains.

As a perspective for future work, we propose to extend this study by formulating and analyzing other epidemic models on directed complex networks. This extension would allow us to reflect on the directionality of real-world contact patterns (see [47]).

References

[1] Aarir, M., Harroudi, S., Allali, K., Danane, J., 2026. Global stability of a fractional two-strain seir model. Gulf Journal of Mathematics 23(1). doi:https://doi.org/10.56947/hp89pj07.

[2] Asamoah, J.K.K., Nyabadza, F., Jin, Z., Bonyah, E., Khan, M.A., Li, M.Y., Hayat, T., 2020. Backward bifurcation and sensitivity analysis for bacterial meningitis transmission dynamics with a nonlinear recovery rate. Chaos, Solitons & Fractals 140, 110237. doi:https://doi.org/10.1016/j.chaos.2020.110237.

[3] Ashrafur Rahman, S., Zou, X., 2011. Flu epidemics: a two-strain flu model with a single vaccination. Journal of Biological Dynamics 5(5), 376–390. doi:https://doi.org/10.1080/17513758.2010.510213.

[4] Baba, I.A., Hincal, E., 2017. Global stability analysis of two-strain epidemic model with bilinear and non-monotone incidence rates. The European Physical Journal Plus 132(5), 208. doi:https://doi.org/10.1140/epjp/i2017-11476-x.

[5] Capasso, V., Serio, G., 1978. A generalization of the kermack-mckendrick deterministic epidemic model. Mathematical biosciences 42(1-2), 43–61. doi:https://doi.org/10.1016/0025-5564(78)90006-8.

[6] Cheng, X., Wang, Y., Huang, G., 2021. Global dynamics of a network-based SIQS epidemic model with nonmonotone incidence rate. Chaos, Solitons & Fractals 153, 111502. doi:https://doi.org/10.1016/j.chaos.2021.111502.

[7] d'Onofrio, A., 2008. A note on the global behaviour of the network-based SIS epidemic model. Nonlinear Analysis: Real World Applications 9(4), 1567–1572. doi:10.1016/j.nonrwa.2007.04.001.

[8] El Haitami, A., 2025. A markovian switching diffusion for an sirs epidemic model on complex network. Gulf Journal of Mathematics 20(2), 253–274. doi:https://doi.org/10.56947/gjom.v20i2.3079.

[9] Fu, T., Li, S., Liu, M., 2025. Dynamics and optimal control of an siqr epidemic model with vaccination and individual feedback on networks. Journal of Applied Mathematics and Computing 71(4), 5651–5668. doi:https://doi.org/10.1007/s12190-025-02453-9.

[10] Goldman, R.C., Plumley, K.V., Laughon, B.E., 2007. The evolution of extensively drug resistant tuberculosis (XDR-TB): history, status and issues for global control. Infectious Disorders-Drug Targets (Formerly Current Drug Targets-Infectious Disorders) 7(2), 73–91. doi:https://doi.org/10.2174/187152607781001844.

[11] Gorbalenya, A., Baker, S., Baric, R.S., de Groot, R., Drosten, C., Gulyaeva, A.A., Haagmans, B., Lauber, C., Leontovich, A.M., Neuman, B.W., et al., 2020. The species severe acute respiratory syndrome-related coronavirus: classifying 2019-ncov and naming it SARS-CoV-2. Nature microbiology 5(4), 536–544. doi:https://doi.org/10.1038/s41564-020-0695-z.

[12] Hale, J.K., Lunel, S.M.V., 2013. Introduction to functional differential equations. volume 99. Springer Science & Business Media. doi:https://doi.org/10.1007/978-1-4612-4342-7.

[13] Itoh, Y., Shinya, K., Kiso, M., Watanabe, T., Sakoda, Y., Hatta, M., Muramoto, Y., Tamura, D., Sakai-Tagawa, Y., Noda, T., et al., 2009. In vitro and in vivo characterization of new swine-origin H1N1 influenza viruses. Nature 460(7258), 1021–1025. doi:https://doi.org/10.1038/nature08260.

[14] Janik, E., Ceremuga, M., Niemcewicz, M., Bijak, M., 2020. Dangerous pathogens as a potential problem for public health. Medicina 56(11), 591. doi:https://doi.org/10.3390/medicina56110591.

[15] Kang, H., Fu, X., 2015. Epidemic spreading and global stability of an SIS model with an infective vector on complex networks. Communications in Nonlinear Science and Numerical Simulation 27(1-3), 30–39. doi:https://doi.org/10.1016/j.cnsns.2015.02.018.

[16] Kermack, W.O., McKendrick, A.G., 1927. A contribution to the mathematical theory of epidemics. Proceedings of the royal society of london. Series A, Containing papers of a mathematical and physical character 115, 700–721. doi:https://doi.org/10.1098/rspa.1927.0118.

[17] Khan, M.M.U.R., Arefin, M.R., Tanimoto, J., 2023. Time delay of the appearance of a new strain can affect vaccination behavior and disease dynamics: An evolutionary explanation. Infectious Disease Modelling 8(3), 656–671. doi:10.1016/j.idm.2023.06.001.

[18] Khyar, O., Allali, K., 2020. Global dynamics of a multi-strain SEIR epidemic model with general incidence rates: application to COVID-19 pandemic. Nonlinear dynamics 102(1), 489–509. doi:https://doi.org/10.1007/s11071-020-05929-4.

[19] Kuddus, M.A., McBryde, E.S., Adekunle, A.I., Meehan, M.T., 2022. Analysis and simulation of a two-strain disease model with nonlinear incidence. Chaos, Solitons & Fractals 155, 111637. doi:https://doi.org/10.1016/j.chaos.2021.111637.

[20] Kuddus, M.A., McBryde, E.S., Adekunle, A.I., White, L.J., Meehan, M.T., 2021. Mathematical analysis of a two-strain disease model with amplification.

Chaos, Solitons & Fractals 143, 110594. doi:https://doi.org/10.1016/j.chaos.2020.110594.

[21] Kuddus, M.A., Meehan, M.T., White, L.J., McBryde, E.S., Adekunle, A.I., 2020. Modeling drug-resistant tuberculosis amplification rates and intervention strategies in bangladesh. PloS one 15(7), e0236112. doi:https://doi.org/10.1371/journal.pone.0236112.

[22] Li, C.H., Tsai, C.C., Yang, S.Y., 2014. Analysis of epidemic spreading of an SIRS model in complex heterogeneous networks. Communications in Nonlinear Science and Numerical Simulation 19(4), 1042–1054. doi:https://doi.org/10.1016/j.cnsns.2013.08.033.

[23] Li, C.L., Cheng, C.Y., Li, C.H., 2023. Global dynamics of two-strain epidemic model with single-strain vaccination in complex networks. Nonlinear Analysis: Real World Applications 69, 103738. doi:10.1016/j.nonrwa.2022.103738.

[24] Li, K., Zhu, G., Ma, Z., Chen, L., 2019. Dynamic stability of an SIQS epidemic network and its optimal control. Communications in Nonlinear Science and Numerical Simulation 66, 84–95. doi:https://doi.org/10.1016/j.cnsns.2018.06.020.

[25] Li, M.Y., Wang, L., 2002. Global stability in some SEIR epidemic models, in: Mathematical approaches for emerging and reemerging infectious diseases: models, methods, and theory, Springer. pp. 295–311. doi:https://doi.org/10.1007/978-1-4613-0065-6_17.

[26] Li, S., Yuan, Y., 2024. Dynamics of two-strain epidemic model with imperfect vaccination on complex networks. Journal of Applied Mathematics and Computing 70(3), 1859–1885. doi:https://doi.org/10.1007/s12190-024-02025-3.

[27] Liu, L., Wei, X., Zhang, N., 2019. Global stability of a network-based SIRS epidemic model with nonmonotone incidence rate. Physica A: Statistical Mechanics and its Applications 515, 587–599. doi:https://doi.org/10.1016/j.physa.2018.09.152.

[28] Liu, Q.M., Deng, C.S., Sun, M.C., 2014. The analysis of an epidemic model with time delay on scale-free networks. Physica A: Statistical Mechanics and Its Applications 410, 79–87. doi:https://doi.org/10.1016/j.physa.2014.05.010.

[29] Liu, W.m., Levin, S.A., Iwasa, Y., 1986. Influence of nonlinear incidence rates upon the behavior of SIRS epidemiological models. Journal of mathematical biology 23(2), 187–204. doi:https://doi.org/10.1007/BF00276956.

[30] Pastor-Satorras, R., 2001. Epidemic Spreading in Scale-Free Networks. Phys. Rev. Lett. 86, 3200–3203. doi:10.1103/PhysRevLett.86.3200.

[31] Pastor-Satorras, R., Vespignani, A., 2001. Epidemic dynamics and endemic states in complex networks. Physical Review E 63, 066117. doi:https://doi.org/10.1103/PhysRevE.63.066117.

[32] Pastor-Satorras, R., Vespignani, A., 2002. Epidemic dynamics in finite size scale-free networks. Physical Review E 65(3), 035108. doi:https://doi.org/10.1103/PhysRevE.65.035108.

[33] Scholtissek, C., Rohde, W.v., Von Hoyningen, V., Rott, R., 1978. On the origin of the human influenza virus subtypes H2N2 and H3N2. Virology 87(1), 13–20. doi:https://doi.org/10.1016/0042-6822(78)90153-8.

[34] Sun, D., Teng, Z., Wang, K., Zhang, T., 2023. Stability and hopf bifurcation in delayed age-structured SVIR epidemic model with vaccination and incubation. Chaos, Solitons & Fractals 168, 113206. doi:https://doi.org/10.1016/j.chaos.2023.113206.

[35] Trauer, J.M., Denholm, J.T., McBryde, E.S., 2014. Construction of a mathematical model for tuberculosis transmission in highly endemic regions of the asia-pacific. Journal of theoretical biology 358, 74–84. doi:https://doi.org/10.1016/j.jtbi.2014.05.023.

[36] Ullah, S., Khan, M.A., Farooq, M., Gul, T., 2019. Modeling and analysis of tuberculosis (tb) in khyber pakhtunkhwa, pakistan. Mathematics and Computers in Simulation 165, 181–199. doi:10.1016/j.matcom.2019.03.012.

[37] Upadhyay, R.K., Pal, A.K., Kumari, S., Roy, P., 2019. Dynamics of an seir epidemic model with nonlinear incidence and treatment rates. Nonlinear Dynamics 96(4), 2351–2368. doi:https://doi.org/10.1007/s11071-019-04926-6.

[38] Vargas-De-León, C., 2011. On the global stability of sis, sir and sirs epidemic models with standard incidence. Chaos, Solitons & Fractals 44(12), 1106–1110. doi:https://doi.org/10.1016/j.chaos.2011.09.002.

[39] Wang, J., Wang, J., Liu, M., Li, Y., 2014. Global stability analysis of an SIR epidemic model with demographics and time delay on networks. Physica A: Statistical Mechanics and its Applications 410, 268–275. doi:https://doi.org/10.1016/j.physa.2014.05.011.

[40] Wang, L., Dai, G.z., 2008. Global stability of virus spreading in complex heterogeneous networks. SIAM Journal on Applied Mathematics 68(5), 1495–1502. doi:https://doi.org/10.1137/070694582.

[41] Wei, X., Zhao, X., Zhou, W., 2022. Global stability of a network-based SIS epidemic model with a saturated treatment function. Physica A: Statistical Mechanics and its Applications 597, 127295. doi:https://doi.org/10.1016/j.physa.2022.127295.

[42] Wu, Y., Zhang, Z., Song, L., Xia, C., 2024. Global stability analysis of two strains epidemic model with imperfect vaccination and immunity waning in a complex network. Chaos, Solitons & Fractals 179, 114414. doi:https://doi.org/10.1016/j.chaos.2023.114414.

[43] Xiang, Y., Jia, Y., Chen, L., Guo, L., Shu, B., Long, E., 2021. COVID-19 epidemic prediction and the impact of public health interventions: A review of COVID-19 epidemic models. Infectious Disease Modelling 6, 324–342. doi:10.1016/j.idm.2021.01.001.

[44] Xu, R., Ma, Z., 2009. Stability of a delayed SIRS epidemic model with a nonlinear incidence rate. Chaos, Solitons & Fractals 41(5), 2319–2325. doi:https://doi.org/10.1016/j.chaos.2008.09.007.

[45] Yang, J., Duan, X., Li, X., 2022. Complex patterns of an SIR model with a saturation treatment on complex networks: An edge-compartmental approach. Applied Mathematics Letters 123, 107573. doi:10.1016/j.aml.2021.107573.

[46] Yang, J., Li, C.H., 2016. Dynamics of a competing two-strain SIS epidemic model on complex networks with a saturating incidence rate. Journal of Physics A: Mathematical and Theoretical 49(21), 215601. doi:https://ioppublishing.org/contacts/.

[47] Yang, P., Jia, J., Shi, W., Feng, J., Fu, X., 2023. Stability analysis and optimal control in an epidemic model on directed complex networks with nonlinear incidence. Communications in Nonlinear Science and Numerical Simulation 121, 107206. doi:https://doi.org/10.1016/j.cnsns.2023.107206.

[48] Yang, P., Wang, Y., 2019. Dynamics for an SEIRS epidemic model with time delay on a scale-free network. Physica A: Statistical Mechanics and its Applications 527, 121290. doi:https://doi.org/10.1016/j.physa.2019.121290.

[49] Yusuf, T.T., Abidemi, A., 2023. Effective strategies towards eradicating the tuberculosis epidemic: An optimal control theory alternative. Healthcare analytics 3, 100131. doi:10.1016/j.health.2022.100131.

[1] Laboratory of Analysis, Geometry and Applications, Faculty of Sciences, Ibn Tofail University, Kenitra, Morocco

Email address: hakim.habri@uit.ac.ma

[2] Scientific Research and Innovation Laboratory (SRILab), High School of Technology, Ibn Tofaïl University, Kenitra, Morocco

Email address: amineelkoufi1@gmail.com

Email address: brahim.fahid@uit.ac.ma